# Crystallographic Characterization of Stepwise Changes in Ligand Conformations as Their Internal Topology Changes and Two Novel Cross-Bridged Tetraazamacrocyclic Copper(II) Complexes

**Timothy J. Hubin,[†] James M. McCormick,[†] Nathaniel W. Alcock,[‡] Howard J. Clase,[‡] and Daryle H. Busch*[,†]**

Chemistry Departments, The University of Kansas, Lawrence, Kansas 66045, and University of Warwick, Coventry CV4 7AL, England

*Received May 6, 1999*

The parallel syntheses of two new cross-bridged tetraazamacrocyclic complexes whose ligands are derived from 1,4,8,11-tetraazacyclotetradecane (cyclam = 14N4) and *rac*-1,4,8,11-tetraaza-5,5,7,12,12,14-hexamethylcyclotetradecane (tetB = $14N4Me_6$) have been characterized through the crystal structure determination of every stepwise intermediate ligand in the multistep ligand syntheses. These structures show that although the final ligand skeletons are nearly identical, the immediate precursors differ greatly because of the six additional methyl groups of the $14N4Me_6$ macrocycle. The inversion from one diastereomer to another of the tetracycle derived from *rac*-$14N4Me_6$ has been chemically induced through the successive addition of methyl groups to the reactive tertiary nitrogens, and the novel heterocycles produced have been crystallographically characterized with one showing a conformation not previously known for these systems. The structures of the two copper(II) complexes have significant geometrical differences, and accordingly, their electrochemical and spectroscopic properties are compared. The complexes exhibit remarkable kinetic stability under harsh conditions.

## Introduction

The metal complexes of tetraazamacrocycles bridged by two-carbon chains across nonadjacent nitrogens have been shown to exhibit exceptional kinetic stability,[1] which is attributed to the enhanced topological constraint within the ligand, a structural feature that makes stepwise donor dissociation difficult.[2] We have extended our studies of these ligand systems to include the diastereoisomers of the hexa-C-methylated 14-membered macrocycle 1,4,8,11-tetraaza-5,5,7,12,12,14-hexamethylcyclotetradecane (Figure 1), to compare their behavior with that of the corresponding unsubstituted, cross-bridged 14-membered macrocycle first prepared by Weisman[3] and recently exploited as a ligand for a wide variety of metal ions.[1,4] The diastereomeric parent macrocycles are commonly assigned the labels tetA and tetB, and they are identified here by the abbreviations *meso*-$14N4Me_6$ and *rac*-$14N4Me_6$, respectively . We now report that the synthesis of the cross-bridged *rac*-$14N4Me_6$ derivative parallels that of unsubstituted cross-bridged 14N4. In addition, we have isolated crystals and obtained X-ray crystal structures of all the new intermediates leading in a stepwise fashion to the cross-bridged *rac*-$14N4Me_6$ ligand, as well as several new structures of the cross-bridged 14N4 precursors and the copper(II) complexes of both ligands. The chemistry and structures of the sequence of precursors for these complexes illuminate the generation of cross-bridged ligand complexes and especially the effect of methyl substitution upon the process. During the preparation of the new cross-bridged ligand derived from the tetA/tetB diastereomers, an unusual inversion of a *rac*-$14N4Me_6$ tetracyclic intermediate was induced through the stepwise addition of methyl groups to the reactive nitrogens. This inversion is not observed in the less sterically crowded unsubstituted 14N4 series and, fortunately, does not prevent the formation of the desired cross-bridged ligand.

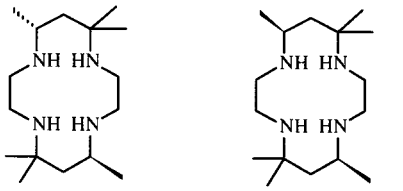


*meso*-$14N4Me_6$ *racemic*-$14N4Me_6$

**Figure 1.** The 14-membered macrocycles *meso*-$14N4Me_6$ (tetA) and *rac*-$14N4Me_6$ (tetB), showing a difference only in the stereochemistry at the site of one of the six methyl substituents.

A short digression is needed to explain the abbreviations applied to the various compounds discussed below. Names based on the root perhydrotetraazapyrene have been given to the tetracyclic tetraamines described in this paper. In an effort to shorten and simplify the following discussion of related structures, we have devised a system of abbreviated names. As indicated above, the common root will be 14N4, a further truncation of the accepted abbreviation [14]aneN4, which identifies the skeleton of the macrocyle that is common to both cyclam and the tetA/tetB diastereomers. The macrocycles tetA

* Corresponding author.
[†] The University of Kansas.
[‡] University of Warwick.

(1) Hubin, T. J.; McCormick, J. M.; Collinson, S. R.; Alcock, N. W.; Busch, D. H. *J. Chem. Soc., Chem. Commun.* **1998**, 1675.
(2) Busch, D. H. *Chem. Rev.* **1993**, *93*, 847. Busch, D. H. Werner Centennial Volume, *ACS Symp. Ser.* **1994**, *565*, 148−164. Busch, D. H. In *Transition Metal Ions in Supramolecular Chemistry*; Fabbrizzi, L., Ed.; Kluwer: Dordrecht, The Netherlands, 1994, pp 55−79.
(3) Weisman, G. R.; Rogers, M. E.; Wong, E. H.; Jasinski, J. P.; Paight, E. S. *J. Am. Chem. Soc.* **1990**, *112*, 8604.
(4) Hubin, T. J.; McCormick, J. M.; Collinson, S. R.; Alcock, N. W.; Kahol, P.; Raghunathan, A.; Busch, D. H. Manuscript in preparation, 1998.

10.1021/ic990491s CCC: $18.00 
Published on Web 09/14/1999

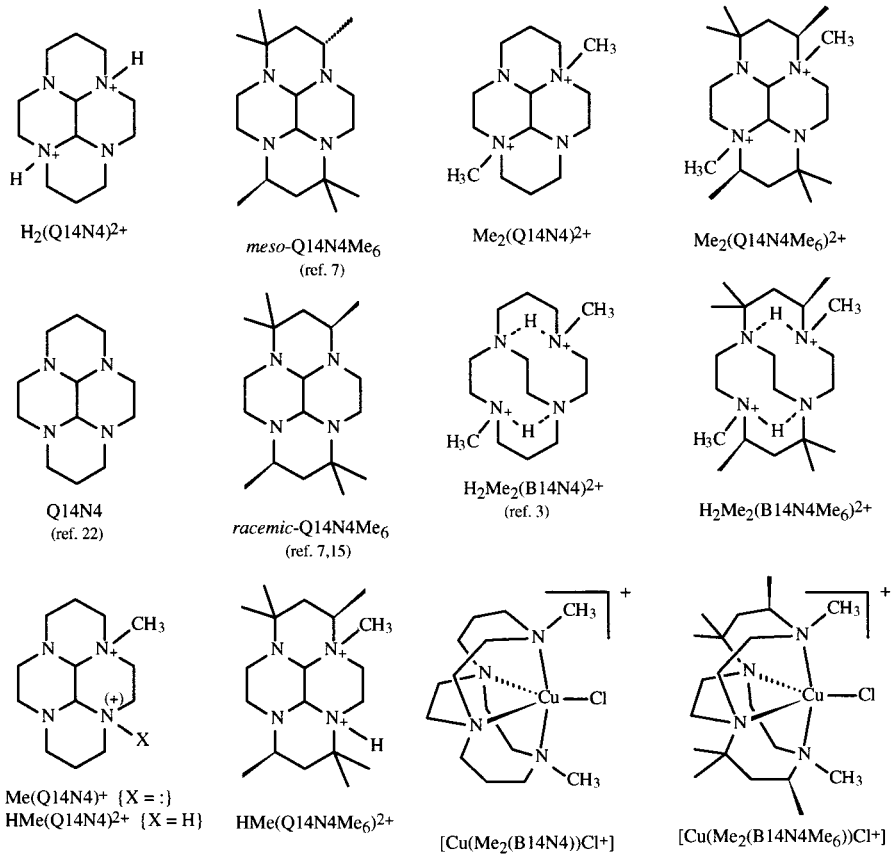


**Figure 2.** Pictorial array of the 13 crystallographically characterized compounds encompassing the stepwise syntheses of the $Cu^{2+}$ complexes of the two closely related cross-bridged ligands discussed in this paper. Nine of the structures are disclosed in this work and provide a very nearly complete presentation of the possible structures for these systems (the other four structures are found in the literature[3,7,15,22]).

and tetB differ only in the relative chirality of one of the monomethylated carbon atoms; tetA is the meso form while tetB is the racemic isomer (see Figure 1). Both are distinguished from 14N4 by the suffix $Me_6$; i.e., tetB is *rac*-14N4$Me_6$ or, when stereochemistry is assumed, simply 14N4$Me_6$. The letter Q will be placed before the 14N4 root to designate the tetracyclic glyoxal condensate of the parent macrocycle (Q14N4), while the letter B will designate the bicyclic cross-bridged species (B14N4). Finally, prefixes (such as $Me_2$ or H) will signify substituents or groups added at nitrogen. For example, HMe-$(Q14N4Me_6)^{2+}$ designates the tetracyclic tetB glyoxal condensate in which one nitrogen has been quaternized by methylation and another nitrogen has been protonated. Figure 2 displays the structures discussed below along with their abbreviations. All but four (whose references are listed below them) are structurally characterized for the first time in this work.

## Experimental Section

**Materials.** Solvents and reagents were of the highest grade available and were found to be sufficiently pure for use as supplied. Where necessary, solvents were dried by prescribed techniques.

**Physical Techniques.** Mass spectra (fast atom bombardment) were obtained using a VG ZAB HS spectrometer equipped with a xenon gun; several matrixes were used, including NBA (nitrobenzyl alcohol) and GLY (glycerol). ESR spectra were recorded on a Bruker ESP300E spectrometer operating in the X-band. Samples were 0.004 M in 1:1 acetonitrile/toluene solutions saturated with tetrabutylammonium hexafluorophosphate. Electrochemical experiments were performed at 25 °C on a Princeton Applied Research model 175 programmer and model 173 potentiostat and used a platinum working electrode, a platinum counter electrode, and a silver reference electrode. The output was recorded on paper using a Houston Instruments recorder. Acetonitrile solutions of the complexes (1 mM) with tetrabutylammonium hexafluorophosphate (0.1 M) as a supporting electrolyte were used in the experiments, which were performed under nitrogen. The potentials vs SHE were determined using ferrocene as an internal reference. NMR spectra were obtained on either a Bruker DRX400 or a QE 300 Plus spectrometer.

**Synthesis of $[H_2(Q14N4)]_2[Fe_2OCl_6]Cl_2\cdot CH_3CN$, Bis(3*a*,8*a*-dihydro-*cis*-10*b*,10*c*-perhydro-1*H*,6*H*-5*a*,10*a*-diaza-3*a*,8*a*-diazoniapyrene) Dichloride (*μ*-Oxo)bis[trichloroferrate(III)] 1-Acetonitrile (1).** Neutral organic Q14N4 was prepared according to literature procedures.[5] The diprotonated salt was the product of an unsuccessful complexation reaction in which 0.35 g (0.0016 mol) of Q14N4 and 0.43 g (0.0016 mol) of $FeCl_3\cdot 6H_2O$ were stirred together for 12 h in 20 mL of acetonitrile. Filtration followed by slow evaporation of the brown filtrate resulted in large brown crystals of the product salt, which were suitable for X-ray diffraction. Yield = 0.58 g (42%). FAB+ mass spectrometry (NBA matrix in acetonitrile) revealed a peak at $m/z$ = 223 corresponding to the monoprotonated ligand cation. Anal. Calcd for $[H_2Q14N4]_2[Fe_2OCl_6]Cl_2\cdot CH_3CN$: C, 34.66; H, 5.71; N, 13.99. Found: C, 34.73; H, 5.60; N, 13.80. An intense, broad band at 855 $cm^{-1}$ in the IR spectrum (KBr disk) is consistent with the Fe−O−Fe antisymmetric stretch[6] and is absent in the spectrum of Q14N4 itself.

**Synthesis of [Me(Q14N4)]I, 3*a*-Methyl-*cis*-10*b*,10*c*-perhydro-1*H*,6*H*-5*a*,8*a*,10*a*-triaza-3*a*-azoniapyrene Iodide (2).** A 6.66 g (0.030 mol) amount of Q14N4 was stirred in 300 mL of dry acetonitrile in a 500 mL three-neck round-bottom flask under $N_2$ at 0 °C. MeI (2 equiv, 0.060 mol, 4.30 mL) was added in one portion by syringe. The reaction mixture was then stirred for 5 min at 0 °C before it was allowed to warm to room temperature and stirred for 2 h more. The white

(5) Weisman, G. R.; Ho, S. C. H.; Johnson, V. *Tetrahedron Lett.* **1980**, 335.
(6) Drew, M. G. B.; McKee, V.; Nelson, S. M. *J. Chem. Soc., Dalton Trans.* **1978**, 80.

precipitate that formed was filtered off, washed with acetonitrile, and dried in vacuo. Yield = 9.06 g (83%). FAB+ mass spectrometry (GLY matrix in water) revealed a single peak at $m/z = 237$ corresponding to $(M - I)^+$. Anal. Calcd for [Me(Q14N4)]I: C, 42.86; H, 6.92; N, 15.38. Found: C, 42.91; H, 6.99; N, 15.41. $^1$H NMR (300 MHz, $D_2O$): $\delta$ 1.34−1.40 (m, 2 H), 1.75−1.86 (m, 2 H), 2.31−2.52 (m, 4 H), 2.83−3.10 (m, 8 H), 3.27 (s, 3 H), 3.37−3.66 (m, 4 H), 3.97 (d, $J = 2.5$ Hz, 1 H), 4.15−4.28 (m, 1 H). $^{13}$C NMR (75.6 MHz, $D_2O$): $\delta$ 18.46, 19.22, 42.55, 46.86, 49.18, 51.67, 52.51, 53.44, 54.31, 65.06, 69.89, 83.26. Crystals suitable for X-ray diffraction were grown by the slow evaporation of water from a saturated solution. The monoprotonated derivative (**3**) was crystallized from a methanol solution to which excess perchloric acid had been added. [**Caution!** Organic perchlorates are potentially explosive and should be prepared and handled with care.]

**Synthesis of [Me$_2$(Q14N4)]I$_2$, 3*a*,8*a*-Dimethyl-*cis*-10*b*,10*c*-perhydro-1*H*,6*H*-5*a*,10*a*-diaza-3*a*,8*a*-diazoniapyrene Diiodide (4).** This compound was synthesized according to literature procedures.[3] Crystals suitable for X-ray diffraction were grown by the slow evaporation of acetonitrile from a saturated solution and contained one acetonitrile of crystallization.

**Synthesis of Me$_2$(B14N4), 4,11-Dimethyl-1,4,8,11-tetraazabicyclo-[6.6.2]hexadecane.** This compound was synthesized according to literature procedures.[3]

**Synthesis of [Cu(Me$_2$(B14N4))Cl]PF$_6$, Chloro(4,11-dimethyl-1,4,8,11-tetraazabicyclo[6.6.2]hexadecane)copper(II) Hexafluorophosphate (5).** Me$_2$(B14N4) (0.27 g, 0.0011 mol) was dissolved in 20 mL of dry MeOH. With stirring, 0.181 g (0.0011 mol) of $CuCl_2 \cdot 2H_2O$ was added as a solid. A green precipitate quickly formed and then redissolved over the next 2 h to give a clear, blue solution. The reaction mixture was then heated to reflux for 10 min. Upon cooling, 0.30 g (0.0018 mol) of $NH_4PF_6$ in 10 mL of MeOH was added and the solution refrigerated for 24 h. The resulting blue precipitate was filtered off, washed with MeOH and ether, and then dissolved in methylene chloride. After filtration, the complex was precipitated by the addition of toluene and washed with toluene and ether before being vacuum-dried. Yield = 0.321 g (64%). FAB mass spectrometry (NBA matrix in methylene chloride) revealed peaks at $m/z = 317$ corresponding to Cu(Me$_2$-(B14N4))$^+$ and $m/z = 352$ corresponding to Cu(Me$_2$(B14N4))Cl$^+$. Anal. Calcd for [Cu(Me$_2$(B14N4))Cl]PF$_6$: C, 33.74; H, 6.07; N, 11.24. Found: C, 33.92; H, 6.14; N, 10.95. Attempts at crystallizing the $PF_6$ salt were unsuccessful. However, if the crude blue MeOH solution was evaporated prior to the $NH_4PF_6$ addition step, recrystallization of the resulting blue solid from $CH_3CN$ gave X-ray-quality crystals of [Cu-(Me$_2$(B14N4))Cl]Cl$\cdot 2H_2O$. All other characterizations were performed on the more easily purified $PF_6$ salt.

**Synthesis of *rac*-[HMe(Q14N4Me$_6$)]I$_2\cdot$CH$_3$CN$\cdot$H$_2$O, *rac*-1,1,3,3*a*,-6,6,8-Heptamethyl-5*a*-hydro-*cis*-10*b*,10*c*-perhydro-8*a*,10*a*-diaza-3*a*,5*a*-diazoniapyrene Diiodide 1-Acetonitrile 1-Hydrate) (6).** Q14N4Me$_6$ (obtained by literature procedures;[7] 3.00 g, 0.01 mol) was dissolved in 70 mL of dry acetonitrile, and the solution was placed in a catalytic hydrogenator bottle modified by the attachment of a female threaded mouth. MeI (15 equiv, 0.15 mol, 10.0 mL) was then added, and the bottle was sealed with a threaded Teflon stopper and immersed in a mineral oil bath. The bath was heated to 100 °C for 24 h. [**Caution!** Sealed reaction vessels may explode. A steel mesh shield was used to surround the reaction bottle which was heated in a hood behind a Plexiglas shield.] The reaction vessel was then cooled to room temperature before removing the Teflon stopper. Filtration yielded a coarse white solid ([Me$_2$(Q14N4Me$_6$)]I$_2$; vide infra), which was washed with 30 mL of acetonitrile and set aside. The brown filtrate, plus acetonitrile washing, was bubbled with nitrogen in a hood for approximately 1 h to remove excess MeI. Allowing the filtrate to stand for several days in a sealed flask yielded the crystalline solid product, which was collected by filtration and washed with a minimum amount of acetonitrile. Yield = 3.21 g (52%). FAB$^+$ mass spectrometry (NBA matrix in water) shows a peak at $m/z = 322$ corresponding to $(M - 2I)^+$. Anal. Calcd for [HMe(Q14N4Me$_6$)]I$_2\cdot$CH$_3$CN$\cdot$H$_2$O: C, 39.70; H, 6.82; N, 11.02. Found: C, 39.99; H, 6.57; N, 10.71. $^1$H NMR (400 MHz, $D_2O$): $\delta$ 0.99 (d, $J = 7$ Hz, 3 H), 1.10 (s, 3 H), 1.15−1.19 (m, 9 H), 1.23 (s, 3 H) 1.26 (dd, 1 H), 1.52 (dd, 1 H), 1.72 (t, $J = 14$ Hz, 1 H), 1.97−2.13 (m, 2 H), 2.29 (m, 1 H), 2.90−3.24 (m, 4 H), 3.39 (s, 6 H), 3.59 (m, 2 H), 3.81 (d, $J = 2.7$ Hz, 1 H), 4.28 (d, $J = 2.7$ Hz, 1 H). $^{13}$C NMR: No acceptable $^{13}$C spectrum was obtained for this molecule, for several contributing reasons. (1) The compound is insoluble in useful NMR solvents except $D_2O$, in which it is only slightly soluble. (2) It appears that the compound undergoes some change over the time required to collect a satisfactory $^{13}$C spectrum; the proton spectrum changes over time in a $D_2O$ solution. (3) The protonated nitrogen is probably partially deprotonated in $D_2O$. Crystals suitable for X-ray diffraction were separated manually from the bulk product crystals and contained 1 equiv of solvated acetonitrile. The air-dried crystals used in the elemental analysis absorbed 1 equiv of water as well.

**Synthesis of [Me$_2$(Q14N4Me$_6$)]I$_2$, *rac*-1,1,3,3*a*,6,6,8,8*a*-Octamethyl-*cis*-10*b*,10*c*-perhydro-5*a*,10*a*-diaza-3*a*,8*a*-diazoniapyrene Diiodide (7).** The coarse white solid set aside in the previous reaction is the pure product. Yield = 1.12 g (20%). FAB+ mass spectrometry (NBA matrix in water) shows small peaks at $m/z = 335$ corresponding to $(M - 2I)^+$ and $m/z = 463$ corresponding to $(M - I)^+$. Anal. Calcd for [Me$_2$(Q14N4Me$_6$)]I$_2$: C, 40.67; H, 6.83; N, 9.49. Found: C, 40.29; H, 7.00; N, 9.10. $^1$H NMR (400 MHz, $D_2O$): $\delta$ 1.21 (d, $J = 4.4$ Hz, 12 H), 1.30 (d, $J = 7.9$ Hz, 6 H), 1.65 (dd, 2 H), 1.96−2.05 (m, 2 H), 2.86−2.95 (m, 2 H), 3.06 (s, 6 H), 3.09 (t, $J = 5.7$ Hz, 2 H), 3.37−3.41 (m, 2 H), 3.64−3.84 (m, 2 H), 4.91 (s, 2 H). $^{13}$C NMR (101 MHz): $\delta$ 14.26, 14.86, 28.44, 37.68, 39.88, 42.73, 43.81, 54.64, 67.19, 74.23. Crystals suitable for X-ray diffraction were grown by the slow evaporation of a half-saturated acetonitrile solution and contained two waters of crystallization.

**Synthesis of Me$_2$(B14N4Me$_6$), *rac*-4,5,7,7,11,12,14,14-Octamethyl-1,4,8,11-tetraazabicyclo[6.6.2]hexadecane (8).** The reductive ring cleavage of the previously described compound was carried out precisely in accord with the literature preparation of Me$_2$(B14N4) from [Me$_2$(Q14N4)]I$_2$.[3] The white solid product required no further purification. Yield = 50−83%. FAB+ mass spectrometry (NBA matrix in methylene chloride) shows only one peak at $m/z = 339$ corresponding to $MH^+$. Anal. Calcd for Me$_2$(B14N4Me$_6$): C, 70.95; H, 12.50; N, 16.55. Found: C, 71.23; H, 12.74; N, 16.40. $^1$H NMR (400 MHz, $CDCl_3$): $\delta$ 0.83 (s, 6 H), 0.89 (d, $J = 8.8$ Hz, 6 H), 1.04 (s, 6 H), 1.19−1.24 (m, 2 H), 1.87−1.99 (m, 4 H), 2.11 (br s, 8 H), 2.23−2.34 (m, 2 H), 2.46−2.52 (m, 2 H), 3.12−3.20 (m, 4 H), 4.58−4.63 (m, 2 H). $^{13}$C NMR (101 MHz, $CDCl_3$): $\delta$ 15.02, 21.29, 31.18, 37.97, 47.11, 51.84, 52.66, 55.31, 56.83, 57.56. Crystals of the diprotonated chloride salt suitable for X-ray diffraction were grown by slow evaporation of acetonitrile from the reaction mixture of an unsuccessful complexation reaction in which $MnCl_2$ was mixed with Me$_2$(B14N4Me$_6$) in acetonitrile. The crystals contained the diprotonated ligand with 2 $Cl^-$ anions and 2.5 water molecules per unit cell.

**Synthesis of [Cu(Me$_2$(B14N4Me$_6$))Cl]Cl$\cdot$H$_2$O, Chloro(4,5,7,7,11,-12,14,14-octamethyl-1,4,8,11-tetraazabicyclo[6.6.2]hexadecane)-copper(II) Chloride 1-Hydrate (9).** Me$_2$B14N4Me$_6$ (0.339 g, 0.001 mol) was dissolved in 10 mL of dry MeOH. A 0.170 g (0.001 mol) sample of $CuCl_2 \cdot 2H_2O$ dissolved in 15 mL of dry MeOH was added to the stirring ligand solution. A green-blue precipitate formed immediately and slowly redissolved over several hours to give a clear emerald-green solution. The crude product was then obtained upon evaporation of the solvent. The pure product was isolated by dissolving the crude green solid in methylene chloride, filtering, and precipitating with ether. Filtration, followed by washing with additional ether, gave the green powder product. Yield = 0.364 g (74%). FAB$^+$ mass spectrometry (NBA matrix in methylene chloride) revealed peaks at $m/z = 401$ consistent with Cu(Me$_2$(B14N4Me$_6$))$^+$ and $m/z = 436$ consistent with Cu(Me$_2$(B14N4Me$_6$))Cl$^+$. Anal. Calcd for [Cu(Me$_2$-(B14N4Me$_6$))Cl]Cl$\cdot$H$_2$O: C, 48.92; H, 9.03; N, 11.41. Found: C, 48.83; H, 8.82; N, 11.10. Crystals suitable for X-ray diffraction were grown by the slow diffusion of ether into a 1:1 methylene chloride/toluene solvent mixture half-saturated with complex and retained the single water molecule of crystallization.

**Decomposition of Cu(L)$^{2+}$.** A 0.1 mM solution of $[Cu(L)Cl]^+$ (L = Me$_2$B14N4, Me$_2$(B14N4Me$_6$)) was prepared in 1 M $HClO_4$. The

(7) Alcock, N. W.; Moore, P.; Mok, K. F. *J. Chem. Soc., Perkin Trans. 2* **1980**, 1186.

**Table 1.** Crystal Data and Structural Refinement Details

| | **1** | **2** | **3** | **4** | **5** |
|---|---|---|---|---|---|
| formula | $C_{26}H_{51}N_9Fe_2OCl_8$ | $C_{13}H_{25}N_4I$ | $C_{13}H_{26}N_4Cl_2O_8$ | $C_{16}H_{31}N_5I_2$ | $CuC_{14}H_{34}N_4Cl_2O_2$ |
| fw | 901.07 | 364.27 | 437.28 | 547.26 | 424.90 |
| space group | $P2_1/n$ | $P2_1/n$ | $P2_1/c$ | $P2_1/c$ | $C2/c$ |
| $a$ (Å) | 11.8765(3) | 11.378(3) | 16.362(2) | 9.748(2) | 29.377(2) |
| $b$ (Å) | 14.9443(5) | 7.103(2) | 9.5980(1) | 13.227(2) | 7.8124(4) |
| $c$ (Å) | 12.3017(4) | 19.263(5) | 12.7870(10) | 16.770(2) | 17.1422(9) |
| $\beta$ (deg) | 115.0360(10) | 103.872(5) | 112.643(2) | 104.921(5) | 101.1810(10) |
| $V$ (Å$^3$) | 1978.23(10) | 1511.7(8) | 1853.3(3) | 2089.4(6) | 3859.5 |
| $Z$ | 4 | 4 | 4 | 4 | 8 |
| $\rho_{calc}$ (g/cm$^3$) | 1.524 | 1.601 | 1.567 | 1.740 | 1.449 |
| $T$ (K) | 293(2) | 180(2) | 180(2) | 180(2) | 180(2) |
| wavelength (Å) | 0.710 73 | 0.710 73 | 0.710 73 | 0.710 73 | 0.710 73 |
| abs coeff (mm$^{-1}$) | 1.305 | 2.110 | 0.401 | 3.017 | 1.422 |
| R1 indices [$I > 2s(I)$] | 0.0645 | 0.0331 | 0.0671 | 0.0222 | 0.0423 |
| wR2 indices (all data)[a,b] | 0.1968 | 0.0726 | 0.1651 | 0.0439 | 0.1181 |

| | **6** | **7** | **8** | **9** |
|---|---|---|---|---|
| formula | $C_{21}H_{41}N_5I_2$ | $C_{20}H_{44}N_4I_2O_2$ | $C_{20}H_{49}N_4Cl_2O_{2.5}$ | $CuC_{20}H_{44}N_4Cl_2O$ |
| fw | 617.39 | 626.41 | 456.53 | 491.03 |
| space group | $P\bar{1}$ | $P2_12_12_1$ | $P2_1/n$ | $P2_1/c$ |
| $a$ (Å) | 10.5080(2) | 9.2565(3) | 10.8025(2) | 14.654(3) |
| $b$ (Å) | 10.9073(2) | 12.4725(5) | 20.7378(2) | 9.910(2) |
| $c$ (Å) | 12.66530(1) | 21.8477(8) | 22.5004(3) | 17.397(3) |
| α (deg) | 80.2190(10) | | | |
| $\beta$ (deg) | 73.5200(10) | | 100.0910(10) | 108.80(2) |
| $\gamma$ (deg) | 66.7520(10) | | | |
| $V$ (Å$^3$) | 1276.20(4) | 2522.4(2) | 4962.57(12) | 2391.5(8) |
| $Z$ | 2 | 4 | 8 | 4 |
| $\rho_{calc}$ (g/cm$^3$) | 1.607 | 1.644 | 1.222 | 1.364 |
| $T$ (K) | 180(2) | 180(2) | 180(2) | 180(2) |
| wavelength (Å) | 0.710 73 | 0.710 73 | 0.710 73 | 0.710 73 |
| abs coeff (mm$^{-1}$) | 2.480 | 2.515 | 0.286 | 1.155 |
| R1 indices [$I > 2s(I)$] | 0.0377 | 0.0322 | 0.0556 | 0.0399 |
| wR2 indices (all data)[a,b] | 0.0833 | 0.0701 | 0.1225 | 0.0991 |

[a] $wR1 = \sum||F_o| - |F_c||/|F_o|$. [b] $wR2 = \{\sum[w(F_o^2 - F_c^2)^2]/\sum[w(F_o^2)^2]\}^{1/2}$. $w = 1/[\sigma^2(F_o^2) + (aP)^2 + bP]$ where $P = (F_o^2 + 2F_c^2)/3$.

**Table 2.** Selected Bond Lengths (Å) and Angles (deg)

| | | | |
|---|---|---|---|
| | $Cu(Me_2(B14N4))Cl^+$ | | |
| Cu(1)−N(12) | 2.093(3) | Cu(1)−N(8) | 2.170(3) |
| Cu(1)−N(5) | 2.108(3) | Cu(1)−Cl(1) | 2.2629(12) |
| Cu(1)−N(1) | 2.107(3) | | |
| N(12)−Cu(1)-N(5) | 175.16(13) | N(1)−Cu(1)-N(8) | 85.30(12) |
| N(12)−Cu(1)-N(1) | 84.74(13) | N(12)−Cu(1)-Cl(1) | 90.60(10) |
| N(5)−Cu(1)-N(1) | 91.22(13) | N(5)−Cu(1)-Cl(1) | 94.16(10) |
| N(12)−Cu(1)-N(8) | 92.04(12) | N(1)−Cu(1)-Cl(1) | 155.82(10) |
| N(5)−Cu(1)-N(8) | 84.96(12) | N(8)−Cu(1)-Cl(1) | 118.63(9) |
| | $Cu(Me_2(B14N4Me_6))Cl^+$ | | |
| Cu(1)−N(8) | 2.114(2) | Cu(1)−N(11) | 2.116(2) |
| Cu(1)−N(4) | 2.128(2) | Cu(1)−N(1) | 2.196(2) |
| Cu(1)−Cl(1) | 2.2939(10) | | |
| N(8)−Cu(1)-N(4) | 92.88(8) | N(11)−Cu(1)-N(4) | 175.14(8) |
| N(8)−Cu(1)-N(1) | 87.51(8) | N(11)−Cu(1)-N(1) | 92.76(8) |
| N(4)−Cu(1)-N(1) | 83.08(8) | N(8)−Cu(1)-Cl(1) | 141.37(6) |
| N(11)−Cu(1)-Cl(1) | 91.21(6) | N(4)−Cu(1)-Cl(1) | 93.42(6) |
| N(1)−Cu(1)-Cl(1) | 131.09(6) | N(8)−Cu(1)-N(11) | 84.39(8) |

absorbance at $\lambda_{max} = 300$ nm (for L = $Me_2$(B14N4)) or $\lambda_{max} = 327$ nm (for L = $Me_2$(B14N4$Me_6$)) was observed over a period of 1000 h (for L = $Me_2$(B14N4)) or 530 h (for L = $Me_2$(B14N4$Me_6$)) at 40 °C to determine the rate of decomposition of the complex under these conditions. Control spectra, for mixtures of 1 equiv of ligand and 1 equiv of $CuCl_2 \cdot 2H_2O$ in 1 M $HClO_4$, were collected and showed no absorbances at the wavelengths studied.

**X-ray Crystallography.** Table 1 lists the crystal data and refinement details for the new structures appearing in this article. Bond lengths and angles as well as atomic coordinates and equivalent isotropic displacement parameters are included in the Supporting Information. For clarity of discussion, selected bond lengths and angles for $Cu(Me_2(B14N4))Cl^+$ and $Cu(Me_2(B14N4Me_6))Cl^+$ are presented in Table 2.

**(a) Data Collection and Processing.** A Siemens SMART three-circle system with a CCD area detector was used.[8] The crystal temperature was maintained with an Oxford Cryosystems Cryostream cooler.[9] Absorption corrections were applied by using $\psi$-scans (except for the case of **1**); crystal decay was checked by re-collection of initial frames and proved to be negligible for all structures.

**(b) Structure Analysis and Refinement.** The space groups were uniquely determined by the systematic absences, apart from those of structures **5** and **6**. The structures were solved by direct methods using SHELXS[10] (TREF) with additional light atoms found by Fourier methods. Hydrogen atoms were added at calculated positions and refined using a riding model. Anisotropic displacement parameters were used for all non-H atoms; H atoms were given isotropic displacement parameters equal to 1.2 times the equivalent isotropic displacement parameter of the atom to which the respective H atom was attached. Refinement used SHELXL 96.[10]

**(c) Specific Comments. 1**: crystal character deep-red blocks. **2**: crystal character colorless bipyramids. The single large peak in the difference Fourier synthesis is at $x$, $^1/_2 - y$, $z$ from the $I^-$ ion. **3**: crystal character colorless blocks. The structure was solved in space group $Pc$ and was then converted to $P2_1/c$. **4**: crystal character colorless plates. The asymmetric unit includes one lattice molecule of acetonitrile. **5**: crystal character green blocks. Systematic absences indicated either space group $C2/c$ or $Cc$. The former was chosen on the basis of intensity statistics and shown to be correct by successful refinement. The lattice contains three water molecules, two lying on 2-fold axes. All the water hydrogen atoms were located on difference maps, and their positions were refined, restraining the O−H distances to be equal. **6**: crystal character colorless blocks. Space group $P\bar{1}$ was chosen on the basis of intensity statistics and shown to be correct by successful refinement.

(8) *SMART User's Manual*; Siemens Industrial Automation Inc.: Madison, WI, 1994.
(9) Cosier, J.; Glazer, A. M. *J. Appl. Crystallogr.* **1986**, *19*, 105.
(10) Sheldrick, G. M. *SHELX-96* ($\beta$-test) (including SHELXS and SHELXL); University of Göttingen: Göttingen, Germany, 1996.

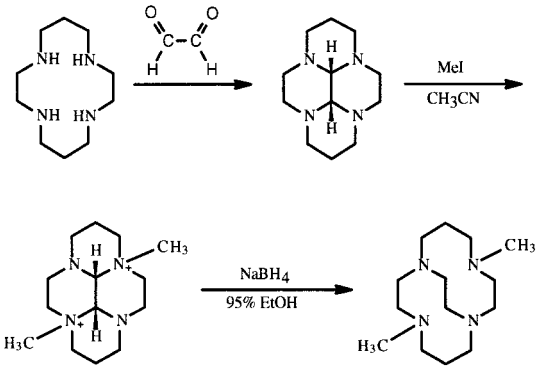


**Figure 3.** Literature procedure[3] for the synthesis of cross-bridged macrocycles, exploiting the cis fusion of the tetracyclic glyoxal condensate for selective alkylation at nonadjacent nitrogens. This allows the ring-opening reduction to form the desired cross-bridged product.

**7**: crystal character colorless blocks. The asymmetric unit contains two lattice water molecules. Possible positions for their H atoms were visible on difference Fourier maps, but they could not be unambiguously identified and were not included. The absolute structure of the individual crystal chosen was checked by refinement of a $\delta f''$ multiplier. Absolute structure parameter $x = 0.60(2)$, indicating that it was an almost complete racemic twin. **8**: crystal character colorless plates. The asymmetric unit contains two cations, four chloride anions, and five water molecules. The hydrogen atoms of the two protonated nitrogen atoms and of the water molecules were all located clearly from Fourier syntheses. Coordinates for the water and protonation hydrogen atoms were refined. **9**: crystal character green plates. The asymmetric unit includes one lattice water molecule. The H atoms of the lattice water were located on a difference Fourier map, and the coordinates were refined with restrained O−H distances.

## Results and Discussion

**Background.** Tetracyclic tetraamines produced from the condensation of glyoxal with various tetraazamacrocycles have been known for more than two decades.[11] Macrocycles possessing several ring sizes and containing various alkyl substituents on ring carbons can undergo this reaction (Figure 3).[5,11] Surprisingly, little use of the reactive tertiary amine groups contained in such structures has been reported, except in the cross-bridging chemistry of Weisman et al.[3] and the coordination of the tetracycles as bidentate ligands to palladium and copper by some of us.[12] The cross-bridging chemistry,[3] an important breakthrough because of the topologically constrained ligands it produced, exploited the cis configuration of the central two-carbon bridge, which imposes a folded geometry on the molecule (Figure 3). That fold forces adjacent nitrogens of the molecule to direct their lone pairs toward opposite faces of the structure, which facilitates selective alkylation of nonadjacent nitrogens and leads to the cross-bridged product upon ring-opening reduction of the quaternary nitrogens.

The quantitative formation (from 14-membered ring systems) of cis-fused tetracycles, as opposed to mixtures of isomers, has been explained by both kinetic[7] and thermodynamic[13] arguments (Figure 4). The former centers on the probability of formation

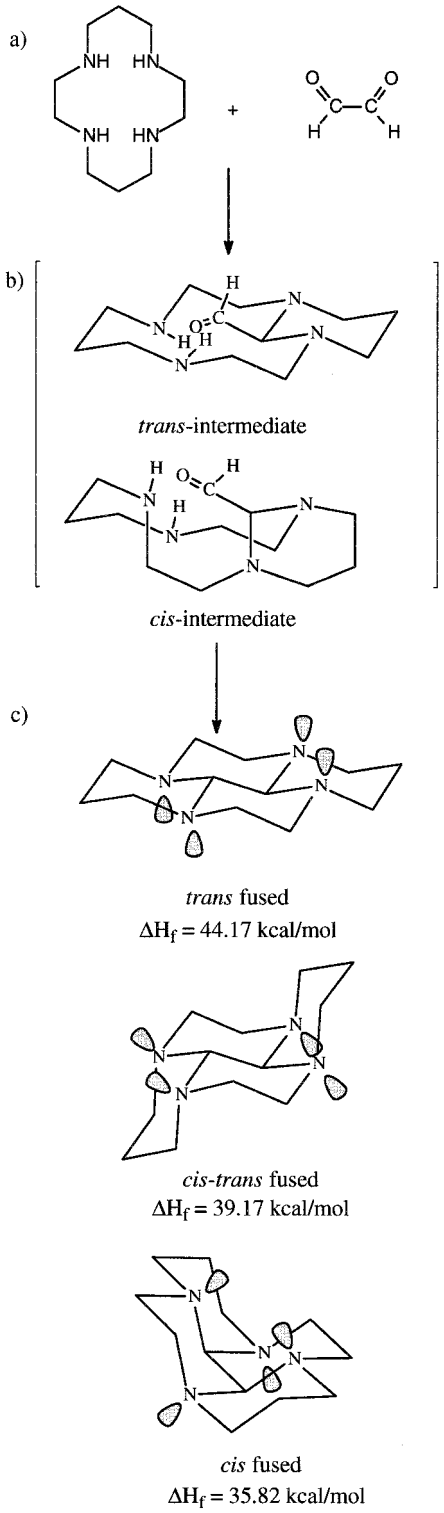


**Figure 4.** (a) Condensation of the macrocycle and glyoxal, resulting in the quantitative synthesis of cis-fused tetracyclic tetraamines. (b) Kinetic control of the preferred product occurring because of steric crowding in the trans intermediate which is not present in the preferred cis intermediate.[7] (c) Thermodynamic control of the preferred cis product, supported by calculated heats of formation, with higher values found for structures having adjacent nitrogens directing their lone pairs to the same face of the molecule.[13]

of intermediates in which one aldehyde of glyoxal has fully reacted with two secondary amines of the macrocycle prior to reaction of the second aldehyde group. The intermediate giving rise to the trans product is sterically very crowded compared to the more open intermediate leading to the cis product (Figure

(11) (a) Choinski, W. M. Ph.D. Thesis, Institute of Organic Chemistry, Polish Academy of Sciences, Warsaw, 1974. (b) Caulkett, P. W. R.; Greatbanks, D.; Turner, R. W.; Jarvis, J. A. J. *J. Chem. Soc., Chem. Commun.* **1977**, 150.

(12) (a) Hubin, T. J.; McCormick, J. M.; Alcock, N. W.; Busch, D. H. *Inorg. Chem.* **1998**, *37*, 6549. (b) Hubin, T. J.; McCormick, J. M.; Alcock, N. W.; Clase, H. J.; Busch, D. H. Manuscript in preparation, 1998.

(13) Okawara, T.; Takaishi, H.; Okamoto, Y.; Yamasaki, T.; Furukawa, M. *Heterocycles* **1995**, *41*, 1023.

4b).[7] The thermodynamic argument centers on MOPAC-calculated heats of formation for the cis, trans and cis−trans isomers. These values indicate that the cis isomer is energetically favored, and this has been attributed to the repulsion between *adjacent* nitrogen lone pairs that are directed to the same face of the molecule in the trans and cis−trans structures. The cis form avoids this interaction by directing adjacent nitrogen lone pairs to opposite sides of the fused-ring system (Figure 4c).[12] No doubt both the kinetic and the thermodynamic effects contribute to the observed dominance of the cis form.

An interesting aspect of these cis-fused tetracyclic structures is their inversion from one enantiomeric form to the other. The unsubstituted tetracycle, Q14N4, has $C_2$ symmetry (axis perpendicular to the ethylene bridge bond) and is therefore chiral. Weisman et al. used this characteristic to explain the temperature-dependent NMR spectra of the molecule and to assign its configuration as cis-fused since the trans-fused isomer cannot undergo inversion without bond breakage.[5] Riddel et al. explored the energetics of this inversion and its probable stepwise path.[14] The activation energy for the inversion process was measured to be 14.95 ± 0.2 kcal/mol at 45 °C. Using several assumptions derived from previous studies on related systems as bases for molecular mechanics calculations, a likely path for the inversion was proposed (Figure 5a): (1) one piperazine ring is transformed from chair to nonchair with an associated nitrogen atom inversion, leading to an asymmetric intermediate; (2) the second piperazine follows suit, leading to a $C_{2v}$ symmetric form; (3) inversion of the remaining two nitrogens in analogous steps yields the enantiomer of the initial diastereomer. Overall, all four nitrogens and both piperazine rings become inverted, and both hexahydropyrimidine rings retain their initial geometric states.[14]

Several other unsubstituted tetracycles of differing ring sizes undergo related inversion processes with similar energies of activation.[14a] Yet no such dynamic process has been reported for systems in which alkyl substituents are appended to the ring carbons. *meso*- and *rac*-14N4Me$_6$ react with glyoxal to form cis-fused tetracycles in analogy to 14N4.[7] But the interconversion between diastereomers has not been directly observed in the case of the tetracycles derived from 14N4Me$_6$. *meso*-Q14N4Me$_6$ has produced only the single cis diastereomer placing the geminal dimethyls at locations "remote" from the fold,[7] while *rac*-Q14N4Me$_6$, as demonstrated by crystal structures, can locate the geminal dimethyls either "close" to the fold or remote from it (i.e., both diastereomers), depending on the synthetic conditions (Figure 6).[7,15] "Close" methyl groups are collinear with the fold; "remote" methyl groups are at the periphery of the folded "wings", on a line perpendicular to the fold.[15] If the inversion process described for the unsubstituted tetracycle Q14N4 were to occur for the Q14N4Me$_6$ systems, the "close" and "remote" methyl positions would be interchanged (Figure 5b). Below, we discuss new observations relating to skeletal inversion, the location of the geminal dimethyl substituents, and the production of cross-bridged ligands from 14N4 and 14N4Me$_6$.

**Ligand and Precursor Structures.** Several different N-substituted cross-bridged ligands, R$_2$(B14N4) (R = H, Me, Bn), and some of their $Li^+$ and $Cu^{2+}$ complexes were previously prepared by Weisman et al.[3,16] Many additional metal complexes

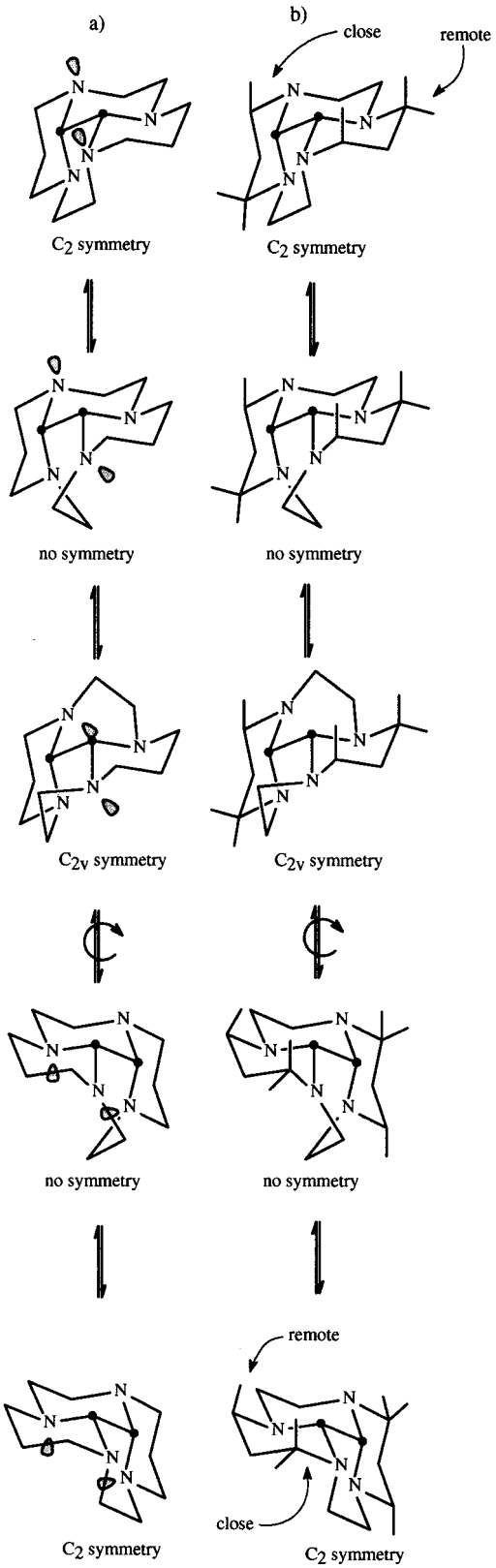


**Figure 5.** Proposed path for the interconversion of enantiomeric forms of Q14N4[14] (a) tracing two lone pairs through the unsubstituted system's inversion and (b) following the hexamethylated tetracycle (*meso*-Q14N4Me$_6$) to show how "close" and "remote" sites interchange during the rearrangement.

of these ligands have been prepared in our laboratories.[1] The reason for successful cross-bridging in the preparation of these ligands was explained on the basis of NMR studies. The explanation focused on the folded structure of the tetracyclic

(14) (a) Kolinski, R. A.; Riddel, F. G. *Tetrahedron Lett.* **1981**, 2217. (b) Riddel, F. G.; Murray-Rust, P.; Kolinski, R.; Gluziński, P. *Tetrahedron* **1982**, *38*, 673.

(15) Gluziński, P.; Krajewski, J. W.; Urbańczyk-Lipkowska, Z.; Bleidelis, J.; Ķemme, A. *J. Crystallogr. Spectrosc. Res.* **1986**, *16*, 271.

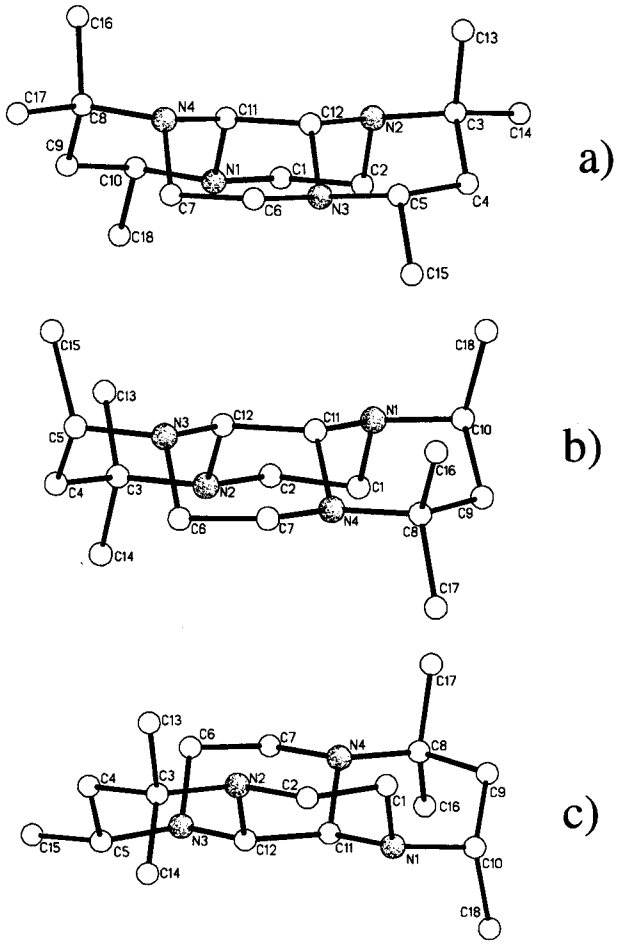


**Figure 6.** Previously characterized diastereomers of Q14N4Me$_6$. (a,b) *rac*-Q14N4Me$_6$ has been prepared in two forms,[7,15] both of which have sterically shielding axial methyl groups a to convex-facing nitrogens. (c) *meso*-Q14N4Me$_6$ has only been characterized in one form,[7] where only one convex-facing nitrogen is blocked by an axial methyl on the a carbon.

glyoxal condensate, in which two nitrogen lone pairs on nonadjacent nitrogens are directed into the concave face of the folded structure while the other two nonadjacent nitrogen lone pairs are directed out from the convex face. From NMR spectra of the dimethylated iodide salt, it was concluded that MeI only adds methyl groups to the convex facing groups to the convex facing nitrogens. Thus, nitrogen atoms having lone pairs pointing inward from the concave face were thought to be sterically unavailable for reaction.[3] This idea was challenged by the crystal structure we obtained in our early studies on $H_2(Q14N4)^{2+}$ (Figure 7a). In this salt, protonation occurs at the two nitrogens having lone pairs pointed into the cleft formed by the folded molecule. This observation led us to suspect that one of these basic nitrogens may, in fact, react with the first methyl group in the methylation reaction since the cleft is not visibly blocked. Molecular models indicate that the cleft should accommodate at least one methyl group. To test this hypothesis, the X-ray crystal structures of the N-mono- and N,N′-dimethylated Q14N4 tetracyclic cations were obtained (Figure 7b,d). Me(Q14N4)I was synthesized by the reaction of Q14N4 with MeI at low temperature in acetonitrile for only a short period of time, whereas the dimethylated salt $Me_2(Q14N4)I_2$ was obtained by literature procedures in which the same reaction was allowed to proceed to completion over 72 h.[3] The white precipitate that separates almost immediately upon initiation of the reaction is the monoquat salt, which can easily be collected in a pure form by filtration or allowed to undergo further reaction with MeI to form the diquat salt. The crystal structures of these two salts confirm (Figure 7b,d) that both the first and second methyl groups add to the convex face of cis-fused, folded tetracyclic Q14N4. The final product is a dication with its two quaternary nitrogen atoms in the outward-facing locations. Fortuitously, this is the stereochemistry that appears necessary for the formation of the desired cross-bridged product upon reductive ring cleavage by sodium borohydride[3] (Figure 7). Interestingly, little change in the overall skeleton of the four fused six-membered rings is observed in the course of the two quaternization reactions.

To examine further the selective positioning of protons and methyl groups on this structural framework, a second crystal structure was obtained for the monomethylated molecule, but with a proton added to a nitrogen atom and, necessarily, a second anion ($[HMe(Q14N4)](ClO_4)_2$, Figure 7c). X-ray-quality crystals were grown by the slow evaporation of a methanol solution of [Me(Q14N4)]I to which excess perchloric acid had been added. [**Caution!** Organic perchlorates are potentially explosive and should be prepared and handled with care.] This structure of the dication is nearly identical to that of the nonprotonated monocation except for the presence of the added proton *which is located in the cleft and is adjacent to the quaternary methylated nitrogen.* This clearly confirms the greater basicity of these *internal* nitrogen atoms (vide infra).

Substitution of methyl groups, and possibly more bulky groups, on the skeleton of the cross-bridged ligands is attractive because of the possibility of enhancing the principal advantage of the cross-bridged ligands. We hypothesized that the resulting ligands should be somewhat more rigid than $Me_2$(B14N4) since the ring substituents should provide additional restrictions on the internal motions necessary to dissociate such ligands from metal ions. Optimistically, we also proposed that methyl substituents on ring carbons might exert only minor influences during the overall reaction sequence leading to the corresponding cross-bridged ligands. Consequently, *meso*- and *rac*-14N4Me$_6$ were prepared according to Hay et al.,[17] and the reactions with glyoxal were carried out under literature conditions.[7] The tetracycles derived from *meso*- and *rac*-14N4Me$_6$ have previously been structurally characterized.[7,15] In our first attempt to extend Weisman's cross-bridging chemistry to these highly substituted macrocycles, the pure tetracycle derived from *meso*-14N4Me$_6$ was treated with methyl iodide. Unfortunately, under all conditions explored, only one nitrogen could be methylated. As described above, selective methylation of Q14N4 occurs at nonadjacent nitrogens because only the two nitrogens with their lone pairs appearing on the convex face of the fold are alkylated.[3] Accepting this conclusion that only these nitrogens undergo alkylation, it is possible to understand why only one methyl can be added to the tetracycle from *meso*-14N4Me$_6$. One need only consider the location and orientation of the *C*-methyl substituents. For one of these available (convex facing) nitrogens, only a single methyl group occupies an α-position and that methyl group has an equatorial orientation, making minimal steric demands on its neighboring nitrogen atom (Figure 6c). In contrast, the single methyl group at the position α to the second available (convex facing) nitrogen has an imposing axial

(16) Weisman, G. R.; Wong, E. H.; Hill, D. C.; Rogers, M. E.; Reed, J. P.; Calabrese, J. C. *J. Chem. Soc., Chem. Commun.* **1996**, 947.

(17) (a) Hay, R. W.; Lawrence, G. A.; Curtis, N. F. *J. Chem. Soc., Perkin Trans. 1* **1975**, 591. (b) Tait, A. M.; Busch, D. H. *Inorg. Synth.* **1978**, *18*, 2.

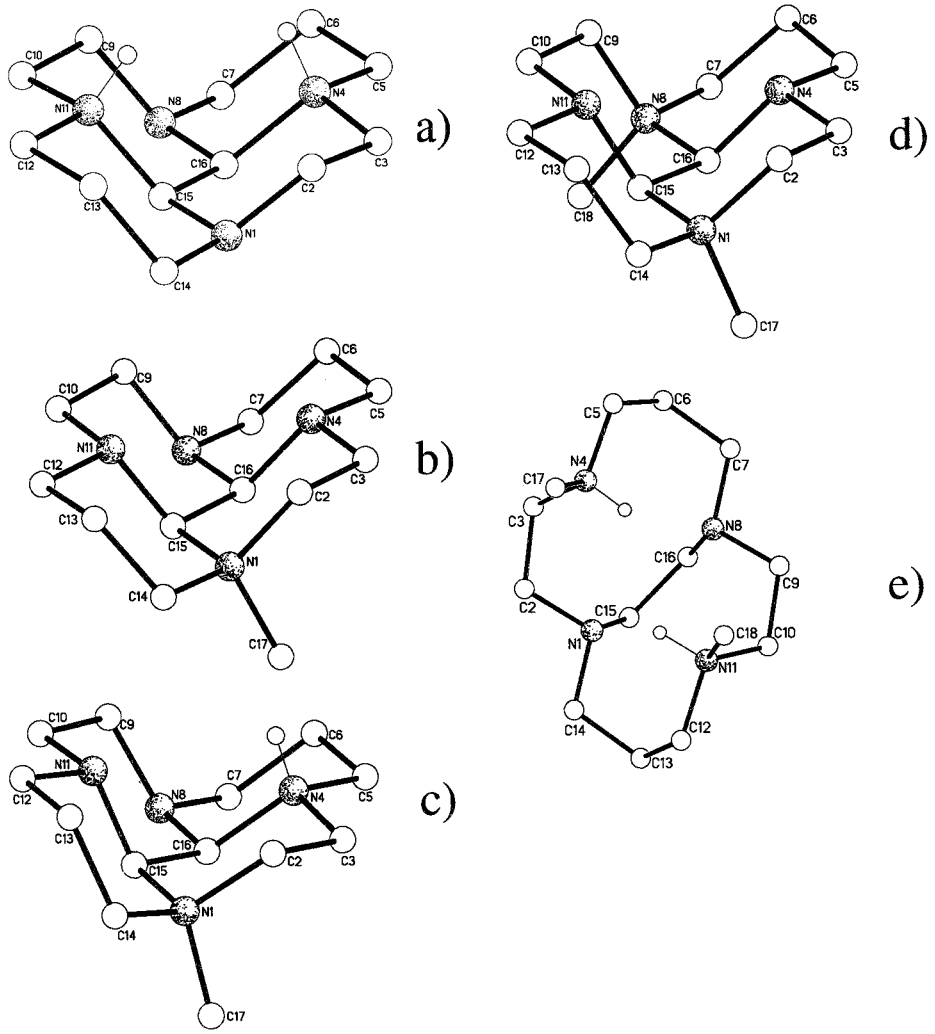


**Figure 7.** New crystal structures of a) $H_2(Q14N4)^{2+}$, (b) $Me(Q14N4)^{+}$, cation and (c) its protonated dication analogue $HMe(14N4Me_6)^{2+}$, and (d) $Me_2(Q14N4)^{2+}$, showing that although the concave-facing nitrogens can be protonated, convex-facing nitrogens are more easily alkylated. This selective alkylation at nonadjacent sites leads to the efficient synthesis of $Me_2(B14N4)$, previously structurally characterized as (e) the diprotonated dication.[3]

orientation, effectively blocking access to the lone electron pair of its adjacent nitrogen atom. The recognition of this structural relationship, along with further failed attempts at methylating the second site using such reactive reagents as dimethyl sulfate and methyl triflate, convinced us that this synthetic pathway to the cross-bridged derivative of *meso*-$14N4Me_6$ should be abandoned.

According to published crystal structures,[7,15] the tetracycle derived from *rac*-$14N4Me_6$, should always have single axial methyl groups, or even worse, geminal dimethyl groups α to the putative reactive, exteriorly directed nitrogen atoms (Figure 6a-b). The two possibilities (single α methyls or geminal α dimethyls) are dependent on which diastereomer of *rac*-$Q14N4Me_6$ is used, making *rac*-$Q14N4Me_6$ an even less likely candidate for the N,N′-dimethylation procedure that is essential to the preparation of cross-bridged ligands by this route. Surprisingly, the reaction of methyl iodide with the corresponding tetracycle (*rac*-$Q14N4Me_6$) gave a small fraction of the dimethylated product under Weisman's conditions, along with the major monomethylated product. By raising the temperature to 100 °C and performing the reaction in a sealed vessel to prevent loss of the volatile acetonitrile and methyl iodide, we obtained a 20% yield of the dimethylated product. Moreover, the monomethylated compound can be recycled to yield another 10% of the desired product. Reductive ring cleavage of this dication via literature conditions[3] gives the cross-bridged ligand $Me_2(B14N4Me_6)$, which was the target of this study. Why the seemingly more sterically crowded *rac*-$Q14N4Me_6$ can be dimethylated when the less crowded *meso*-$Q14N4Me_6$ can only be monomethylated is a substantial question and it is addressed below.

Crystal structures were obtained for the sequentially formed mono- and dimethylated intermediates (Figure 8b,c) and for the target ligand, $Me_2(B14N4Me_6$ ) (Figure 8d). This series of structures provides further insight into the formation of cross-bridged ligands as well as their nitrogen-substituted tetracyclic precursors. The skeletal structure of $HMe(Q14N4Me_6)^{2+}$ (Figure 8b) is virtually identical to the most common form of the *rac*-$Q14N4Me_6$ itself (Figures 6a, 8a),[7] having the familiar cis-fused set of four six-membered rings in chair conformations and the geminal dimethyls in the "close" arrangement. Intriguingly, the structure locates the new *N*-methyl group inside the cleft of the tetracycle, suggesting that the two convex facing nitrogen atoms *are* effectively blocked from alkylation by their neighboring axial methyl groups, which forces the new methyl group to add to the site inside the concave fold. Ironically, we had already come to believe that these internal nitrogens are stronger nucleophiles because they are the preferred protonation sites in Q14N4. Clearly this concave location is not sterically precluded from methylation, as suggested by Weisman.[3] It also appears

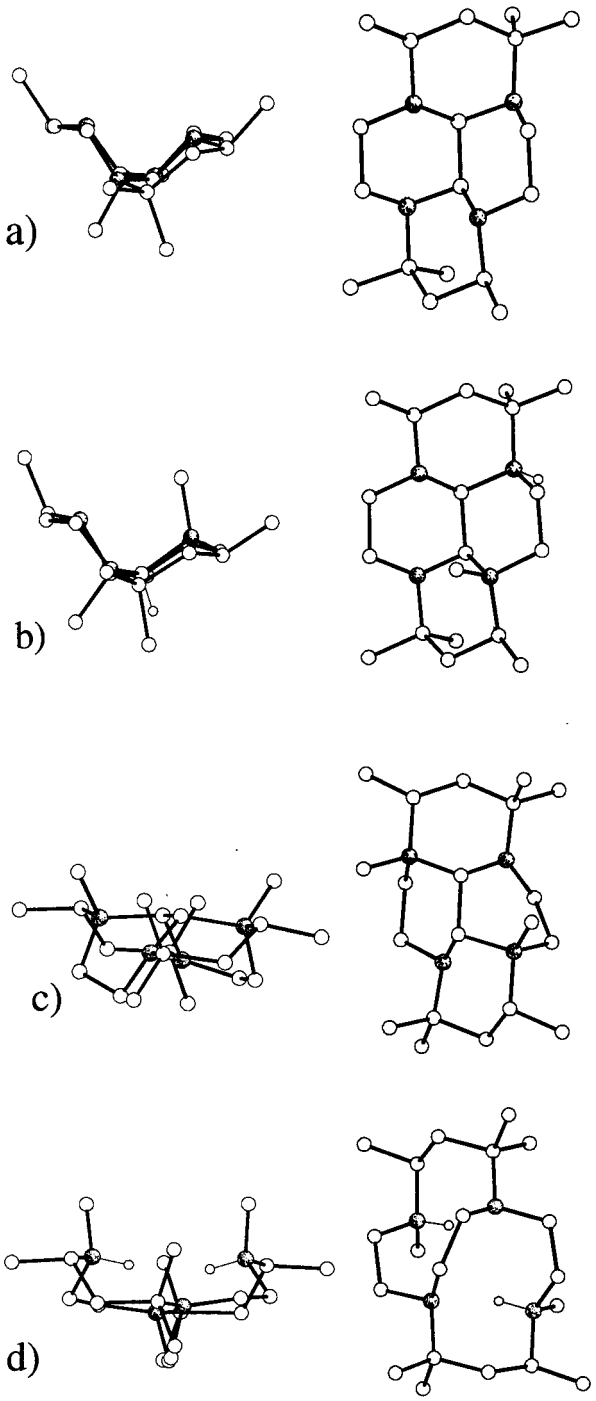


**Figure 8.** (a) Previously structurally characterized *rac*-Q14N4Me$_6^{2+}$,[7] which is not greatly perturbed by (b) the addition of a methyl group to a concave-facing nitrogen, resulting in the HMe(Q14N4Me$_6$)$^{2+}$. However, addition of a second methyl group to the nonadjacent site results in major deformations of the tetracyclic structure (c) including the inversion of the entire tetracyclic structure and the change in conformation of one ring from chair to boat in Me$_2$(Q14N4Me$_6$)$^{2+}$. Strain is apparently relieved as reduction leads to (d) the Me$_2$(B14N4Me$_6$) ligand, structurally characterized as the diprotonated dication and having a conformation identical to that of the unsubstituted Me$_2$(B14N4) diprotonated dication (see Figure 7e).

appropriate to conclude that the energy penalty for placing the substituent in this location is small since the basic skeleton of this tetracycle is essentially unchanged from that of the reactant.

Remarkably, the site preference for protons is also reversed in HMe(Q14N4Me$_6$)$^{2+}$ compared to HMe(Q14N4)$^{2+}$. In fact the proton, in the dication of this monomethylated species is located on an adjacent, convex-facing nitrogen, apparently the more basic, if not more nucleophilic, site.

As described above, the crystal structure of HMe(Q14N4)$^{2+}$ (Figure 7c), which was isolated under acidic conditions (vide supra), locates its proton inside the cleft (concave-facing nitrogen) adjacent to the external (convex facing) methylated nitrogen. These two structures contrast in the concave/convex locations of the proton, as well as the *N*-methyl group, but are alike in that the added proton is found on a nitrogen adjacent to the methylated quaternary nitrogen. This shows that the separation of the two positive charges is not the dominant factor in determining the most basic site in the monocationic free base in either case. Yet, as noted above, the diprotonated H$_2$-(Q14N4)$^{2+}$ structure (Figure 7a) has both protons inside the cleft and on nonadjacent nitrogen atoms. Clearly, assignment of relative basicity and nucleophilicity of these tetracyclic tetraazamacrocycle nitrogen atoms is not simple. In H$_2$(Q14N4)$^{2+}$ and according to Figure 7a,c, the concave-facing nitrogens are more basic, but the convex-facing nitrogens are more successful nucleophiles (Figure 7b,d). The trend is apparently reversed in HMe(Q14N4Me$_6$)$^{2+}$ (Figure 8b). We conclude that steric bulk on the convex side is responsible for the methyl group adding to the concave face (vide supra) and that the resulting structure changes the electronic relationships within the molecule, making the adjacent, convex-facing nitrogen most basic.

Turning to the structure of the dimethylated tetracycle *rac*-Me$_2$(Q14N4Me$_6$)$^{2+}$, models suggest that forcing a second methyl group onto the remaining internal (concave facing) nitrogen would almost certainly require distorting the very rigid molecular skeleton. A methyl group in that second internal site would be confronted with an axial methyl group at an α position and substantial repulsion from the other *N*-methyl group; i.e., two internal *N*-methyl groups would be canted inward toward each other (Figure 8b,c). The structure of the final product in the series, the protonated cation of the targeted cross-bridged ligand Me$_2$(B14N4Me$_6$) (Figure 8d), proves that the second methyl group *must* add at the nonadjacent site. This structure is very similar to that of H$_2$Me$_2$(B14N4)$^{2+}$ as reported by Weisman[3] (Figure 7e), having two protons inside the cavity, each bound to one of the nitrogens and hydrogen bonded to another. This constitutes a demonstration that the second methyl group adds to the tetracycle in a place that is sterically unfavorable, and the structure of the dimethylated tetracycle, Me$_2$(Q14N4Me$_6$)$^{2+}$, can be used to deduce what conformational changes are required (Figure 8c). As anticipated, a *major* deformation of the tetracyclic skeleton takes place in order to accommodate the second methyl group. It is immediately obvious that one of the piperazine rings has undergone a conformational change from chair to boat, analogous to the first step in the enantiomeric interconversion process for Q14N4 (vide supra). To our knowledge, this is the first Q14N4 structure in which all four rings are not in the favored chair conformation. On closer inspection of the structure, it is also apparent that the molecular skeleton has taken on a new conformation; Me$_2$(Q14N4Me$_6$)$^{2+}$ folds on a line approximately perpendicular to the fold in HMe-(Q14N4Me$_6$)$^{2+}$. The geminal dimethyls that occupied "close" positions in the parent tetracycle, Q14N4Me$_6$[7] (Figure 8a), and in the monomethylated species, HMe(Q14N4Me$_6$)$^{2+}$ (Figure 8b), now occupy "remote" locations, and the methyl groups of the quaternary nitrogens now reside at the convex face of the cis-fused structure, despite the fact that the first methyl group is known to have added at the concave face of the parent tetracycle. These observations lead to the inescapable conclusion that the overall skeleton of the tetracycle has been converted from one

diastereomeric form to the other, a process observed for Q14N4 in dynamic NMR experiments (see Background section and Figure 5) but not observed previously for the hexamethylated homologue. Yet in the ultimate cross-bridged product, the geminal dimethyls revert to what once was the fold (Figure 8d), in the so-called "close" positions (this is a result of the ring opening reduction reaction, which necessarily cleaves the C−N bonds of the quaternary nitrogens). The general motion that describes the transformation of the skeleton that accompanies progress through these three structures (Figure 8b,d) resembles the wing motion of a butterfly in flight. Perhaps, more accurately, the change from the fold in the dimethylated structure to the approximately perpendicular fold in the monomethylated and cross-bridged products might better be envisioned as the inversion of a saddle shape. However labeled, a truly remarkable inversion rearrangement is forced upon the tetracyclic skeleton by chemical change—the addition of the second methyl group—rather than through the application of heat, as has been observed for Q14N4.

As noted above, *meso*-Q14N4Me$_6$ can only be mono-N-methylated under ordinary chemical conditions. Why should this seemingly less sterically crowded diastereomer (vide supra) behave in this manner, when the more sterically constrained *rac*-Q14N4Me$_6$ can be di-N-methylated? The structures **6a**−**c** and **8b**−**c** may help us understand this paradox. *meso*-Q14N4Me$_6$ has one available convex-facing nitrogen, and this is the site of monomethylation (Figure 6c). The racemic diastereomer has no sterically available convex-facing nitrogens, and therefore is monomethylated inside the concave fold (Figures 6a and 8b). As shown in Figure 8c, the dimethylation step for *rac*-Q14N4Me$_6$ occurs through inversion of the tetracycle and results in two convex-facing methyl groups. Obviously, having two concave-facing *N*-methyl groups is highly unfavorable and should produce an inversion process (Figure 8c). If *meso*-Q14N4Me$_6$ is monomethylated at the unblocked nitrogen on the convex face (Figure 6c) and its second convex-facing nitrogen is sterically blocked by the axial methyl at the α-carbon (vide supra), then either the second methyl would have to add at an adjacent nitrogen inside the fold (adjacent methylation has never been observed in this family of tetracycles) or the tetracycle must invert, relieving steric bulk from the α-methyl group (which would become equatorial) but placing both *N*-methyl groups inside the fold, an arrangement not favored in any previously determined structure, e.g., Figure 8c. Ironically, the "open" first convex site reacts easily in the case of *meso*-Q14N4Me$_6$, but this reaction effectively *shuts off further methylation*. In *rac*-Q14N4Me$_6$, the first methyl goes in a less favored concave site, yet *inversion is possible to "open up" the second site* on a convex nitrogen.

**Copper Complexes.** Copper(II) complexes of the ligands Me$_2$(B14N4) and Me$_2$(B14N4Me$_6$) were obtained by their reaction with $CuCl_2 \cdot 2H_2O$ in MeOH. Both complexes have been characterized by elemental analysis, mass spectrometry, and X-ray crystallography. Both structures reveal pentacoordinate $Cu^{2+}$ bound to four nitrogen donors from the cross-bridged ligand and a single chloride (Figure 9, Table 2). Both ligands adopt cavity-like conformations engulfing the metal ion, as observed in two earlier structures for $Cu^{2+}$ complexes with related ligands[16] and in a wide variety of complexes involving other metal ions and cross-bridged ligands of this general class (various ring sizes but dimethylene cross-bridges).[1,4] The Me$_2$-(B14N4) complex (Figure 9a) is best described as tetragonal, having the chloride and three nitrogens in a nearly planar arrangement, while the fourth nitrogen donor is at the apex of

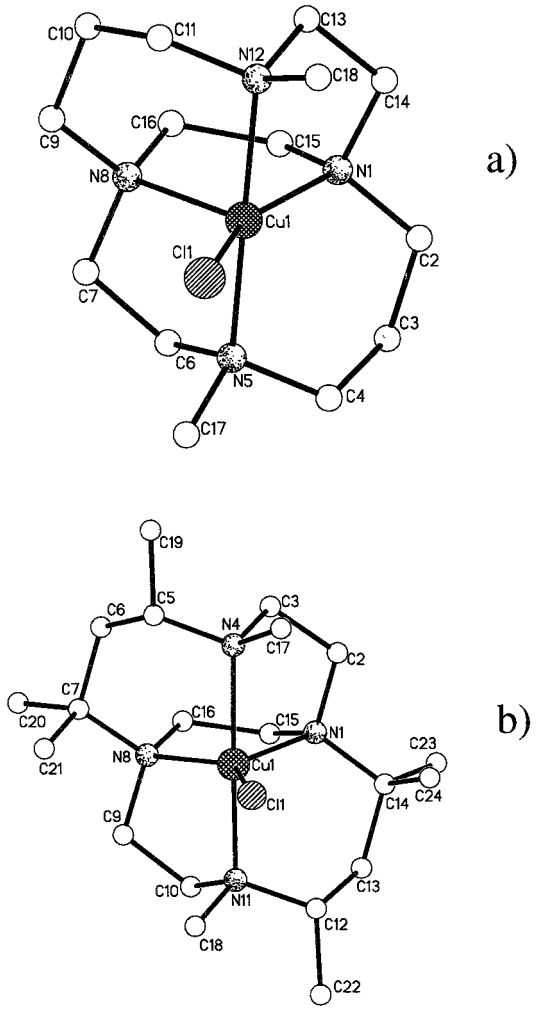


**Figure 9.** Crystal structures of (a) Cu(Me$_2$(B14N4))Cl$^+$ and (b) Cu(Me$_2$(B14N4Me$_6$))Cl$^+$, exhibiting metal ions similarly engulfed in their tetradentate bicyclic ligands. A slight difference in the location of the bound chloride ligands causes a difference in the coordination geometries: (a) is more nearly tetragonal while (b) is trigonal bipyramidal.

the square pyramid. The reason for this structure rather than the expected trigonal bipyramid is unclear, although steric requirements of the ligand should not eliminate either possible geometry. The trigonal bipyramidal geometry is, however, observed for the Me$_2$(B14N4Me$_6$) complex (Figure 9b), where two nitrogen donors from the macrobicycle occupy the axial positions while the other two nitrogens and a chloride fill the three equatorial sites. The difference between the two structures can be readily traced to the six *C*-methyl groups of the Me$_2$-(B14N4Me$_6$) ligand. The two sets of geminal dimethyl groups α to equatorial nitrogen donors N(1) and N(8) in Figure 9b approach the chloride ligand no closer than 3.0 Å in this trigonal bipyramidal structure. However, if a square pyramidal geometry was enforced on this complex, CAChe molecular modeling has shown the distance between chloride and one of the geminal dimethyl groups would have to be about 2.4 Å, clearly an unfavorable proximity. The two previously published[16] $Cu^{2+}$ structures of related R$_2$B14N4 ligands similar in bulk to Me$_2$-B14N4 find $Cu^{2+}$ in geometries also distorted toward square pyramidal and away from trigonal bipyramidal. One has a pseudooctahedral geometry where the sixth ligand involves an agostic interaction with a benzyl hydrogen at a distance of 2.74 Å and the other is five-coordinate and significantly closer in structure to a square pyramid (equatorial angles 87.8(2), 122.0-

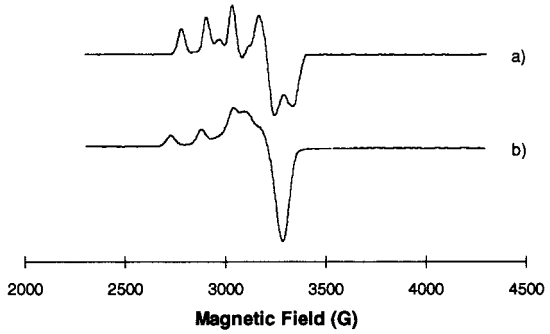


**Figure 10.** X-band EPR spectra of (a) $[Cu(Me_2(B14N4Me_6))Cl]Cl\cdot H_2O$ and (b) $[Cu(Me_2(B14N4))Cl]PF_6$ in 1:1 acetonitrile/toluene solutions. (The solutions were saturated with tetrabutylammonium hexafluorophosphate to sharpen the otherwise broadened signals.)

(1), and 150.2(2)°) than is $[Cu(Me_2B14N4Me_6)Cl]^+$ (equatorial angles 87.51(8), 131.09(6), 141.37(6)°). From these four related structures it may be concluded that, for a nonsterically crowded ligand with the cross-bridged $N_4Cl$ donor set (i.e., $Me_2B14N4$), $Cu^{2+}$ apparently favors a square pyramidal geometry but that the steric bulk of $Me_2B14N4Me_6$ forces the trigonal bipyramidal geometry on copper. Selected metrical parameters for the two structures can be found in Table 2.

Cyclic voltammetry at a scan rate of 200 mV/s in 1 mM acetonitrile at 25 °C showed one irreversible reduction process for each complex, at −0.544 V for $Cu(Me_2(B14N4))Cl^+$ and at −0.475 V ($Cu^{2+}/Cu^+$) for $Cu(Me_2(B14N4Me_6))Cl^+$ versus SHE. The reduction of each $Cu^{2+}$ complex to a $Cu^+$ complex is unremarkable, but the return oxidation wave is sensitive to scan rate in both cases. At high scan rates, the $Cu^+ \rightarrow Cu^{2+}$ oxidation is broadened, indicating coupled chemical events. However, at slow scan rates, the oxidation wave narrows. This behavior indicates that the reduced complexes may exist as mixtures of at least two species, which quickly equilibrate. From the crystal structure of a related $Cu^+$ complex,[18] it appears possible for these $Cu^+$ complexes to exist in four-coordinate forms. Therefore these systems may consist of equilibrium mixtures of four- and five-coordinate $Cu^+$ complexes. The $Me_2(B14N4Me_6)$ complex appears to undergo this equilibration more rapidly than the $Me_2(B14N4)$ complex, as would be expected for the sterically more crowded structure.

The electronic spectra of the complexes were obtained on acetonitrile solutions. Both complexes present the expected ligand field transitions for $d^9$ $Cu^{2+}$. $Cu(Me_2(B14N4))Cl^+$ exhibits a charge-transfer band at $\lambda_{max} = 292$ nm ($\epsilon = 5830$ $M^{-1}$ $cm^{-1}$) and a d−d transition at $\lambda_{max} = 671$ nm ($\epsilon = 100$ $M^{-1}$ $cm^{-1}$). The $Cu(Me_2(B14N4Me_6))Cl^+$ complex has its charge-transfer band at $\lambda_{max} = 311$ nm ($\epsilon = 5140$ $M^{-1}$ $cm^{-1}$) and a d−d band at $\lambda_{max} = 750$ nm ($\epsilon = 240$ $M^{-1}$ $cm^{-1}$). These bands have proven useful in the study of the kinetic stabilities of the complexes (vide infra).

The EPR spectra of the two complexes (Figure 10) feature much greater differences than are found in their electrochemistry or electronic spectra. $[Cu(Me_2(B14N4))Cl]PF_6$ exhibits a signal typical in appearance for $Cu^{2+}$. Rudimentary simulation studies show it to most likely be a rhombic signal, but accurate Hamiltonian parameters have not yet been calculated. In contrast, $[Cu(Me_2(B14N4Me_6))Cl]Cl\cdot H_2O$, in the same solvent system, shows a much more complex spectrum. Simple simulation studies indicate that this is a reversed spectrum in which $g_\perp > g_\parallel$, which is consistent with the trigonal bipyramidal geometry shown in the crystal structure.[19] The simulations also show that the signal is likely due to an overlap of two different signals, one of minor contribution only. Complete assignment of the parameters for these two spectra are beyond our current capabilities and are perhaps best left to a later study.[20]

Probably the most interesting property of these cross-bridged tetraazamacrocycle copper complexes is their remarkable kinetic stability under classically harsh conditions.[21] The behavior of $Cu(Me_2(B14N4))^{2+}$ has been reported previously.[1] Now, studies on the hexamethylated homologue $Cu(Me_2(B14N4Me_6))^{2+}$ confirm that this stability is due to the short cross-bridge. Copper(II), known for forming the most thermodynamically stable yet most kinetically labile divalent transition metal complexes,[22] provides a fascinating insight into the stabilities of the metal complexes of these ultrarigid ligands. The UV−vis spectrum of a 0.1 mM solution of $Cu(Me_2(B14N4))^{2+}$ in 1 M $HClO_4$ remains essentially unchanged over 1000 h at 40 °C; from estimated errors, the lower limit of the half-life for ligand dissociation is >6 years (pseudo-first-order rate constant of dissociation = $3.5 \times 10^{-9}$ $s^{-1}$). This is to be compared with the classic experiments[19] with $Cu(meso\text{-}14N4Me_6)^{2+}$. A blue isomer, believed to contain *meso*-14N4Me$_6$ in the folded form, similar to that forced by our cross-bridged ligands, lost its ligand in 6.1 M HCl with a half-life of about 3 min at 25 °C. Replacement of the six *C*-methyls in *meso*-14N4Me$_6$ by two *N*-methyl groups and the short two-carbon cross-bridge in $Me_2(B14N4)$ has increased the kinetic stability of the corresponding complex by something like 6 orders of magnitude, or more. Even the square planar red isomer of $Cu(meso\text{-}14N4Me_6)^{2+}$ is much more labile than the folded bridged cyclam complex, showing a half-life of 22 days in 6.1 M HCl at 25 °C, making it at least 100 times more labile than $Cu(Me_2(B14N4))^{2+}$. Another appropriate comparison to illustrate the kinetic stabilization imparted by the cross-bridge is that of $Cu(Me_2(B14N4))^{2+}$ with $Cu(tmc)^{2+}$ (tmc = 1,4,8,11-tetramethylcyclam) whose unbridged ligand is most similar to $Me_2B14N4$ (14-membered tetraazamacrocycle with all tertiary nitrogens). The half-life of this complex at 25° in 1 M $HNO_3$ (calculated from the experimentally determined rate law[23]) is only 2 s, or 8 orders of magnitude smaller than that of $Cu(Me_2(B14N4))^{2+}$. Further, it must be emphasized that 6 years is the lower limit of the half-life for the loss of ligand from $Cu(Me_2(B14N4))^{2+}$ in 1 M $HClO_4$; the actual half-life is almost certainly substantially longer. A parallel experiment carried out on the $Cu(Me_2(B14N4Me_6))^{2+}$ complex under the same conditions over 530 h demonstrated a similar stability. In this case, the half-life can be estimated at >8 years (pseudo-first-order rate constant of dissociation = $2.5 \times 10^{-9}$ $s^{-1}$). Despite the absence of exhaustive experiments, we conclude that the half-lives of these compounds, in media that would instantly destroy most typical $Cu^{2+}$ complexes, is of the order of years.

A final pair of comparisons is useful. The Springborg group has produced kinetically inert $Cu^{II}$ complexes of a trimethylene cross-bridged cyclen (Figure 11a).[24,25] The crystal structure

(18) Hubin, T. J.; Alcock, N. W.; Busch, D. H. Manuscript in preparation, 1998.

(19) Bencini, A.; Gatteschi, D. ESR Spectra of Metal Complexes of the First Transition Series in Low-Symmetry Environments. In *Transition Metal Chemistry*; Melson, G. A., Figgis, B. N., Eds.; Marcel Dekker: New York; Vol. 8, 1982; pp 1−178.

(20) The authors thank the reviewers for pointing out the complexity of the EPR spectra.

(21) Cabbiness, D. K.; Margerum, D. W. *J. Am. Chem. Soc.* **1970**, *92*, 2151.

(22) Irving, H.; Williams, R. J. P. *J. Chem. Soc.* **1953**, 3192.

(23) Hertli, L.; Kaden, T. A. *Helv. Chim. Acta* **1974**, *57*, 1328.

(24) Gluziński, P.; Krajewski, J. W.; Urbańczyk-Lipkowska, Z.; Bleidelis, J.; Ķemme, A. *Acta Crystallogr.* **1982**, *B38*, 3038.

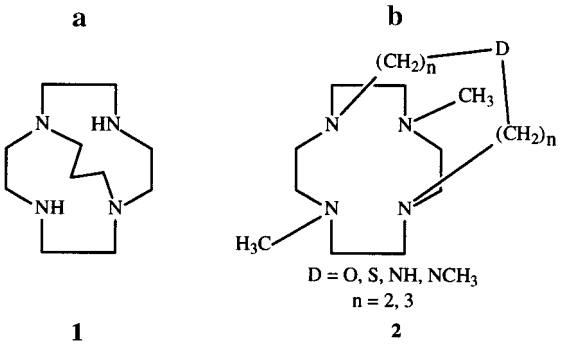


**Figure 11.** (a) Trimethylene-bridged cyclen.[25] (b) The family of bridged cyclens having longer bridging chains containing a fifth donor atom.[26]

shows a coordination geometry similar to that of the present complexes, a macrobicycle-engulfed copper ion with a labile fifth ligand and a geometry intermediate between trigonal bipyramidal and square pyramidal. Kinetic studies in 5 M HCl reveal a first-order dissociation constant at 25 °C for the macrobicycle in $CuLCl^+$ of $1.48 \times 10^{-6}$ $s^{-1}$ (or a half-life of over 5 days). Though an impressive number, it is still some 3 orders of magnitude less stable than the dimethylene cross-bridged complexes of the present study. The likely reasons for our improved stability are better size complementarity for the $Cu^{II}$ ion by the larger parent macrocycles and greatly improved rigidity of the bound ligand, apparently due to decreasing the length of the cross-bridge by one carbon atom, from trimethylene to dimethylene.

Extensive bridging of cyclen with a chain that contains a fifth donor atom has been done (Figure 11b). The resulting five-coordinate $Cu^{II}$ complexes exhibit stabilities similar in strongly acidic conditions to those reported here, although dissociation rates have not been quantified.[26] Even though the bridging group is longer (providing less rigidification) in these examples, addition of a fifth donor, and the associated extra chelate rings, could explain why these complexes are approximately as stable as those with the present ligands.

**Summary.** A new cross-bridged ligand, $Me_2$(B14N4$Me_6$), has been synthesized by adapting literature methodology to a more sterically crowded, highly substituted tetraazamacrocycle. X-ray crystallographic characterization of the sequence of precursor ligands leading to this new cross-bridged macrocycle, and to the corresponding known unsubstituted ligand, $Me_2$-(B14N4), reveals a number of important relationships. In the absence of substituents, N-methylation of the tetracyclic intermediate produced by condensation of glyoxal with the tetraazamacrocycle occurs on two of the nitrogen atoms that have their lone electron pairs pointing away from the cleft in the folded structure while protonation occurs at the nitrogen atoms whose lone pairs point into the cleft. Because of the steric blockage afforded by the arrangement of the six methyl groups, the tetracycle derived from *meso*-14N4$Me_6$ can only be N-monomethylated by typical electrophilic reagents under moderate conditions, and methylation probably occurs at an externally oriented nitrogen. Surprisingly, *rac*-Q14N4$Me_6$, whose externally focused nitrogen atoms are more sterically hindered than those of the *meso* isomer, gives both a dimethylated and a monomethylated derivative. Further, the methyl groups are added to nitrogen atoms whose lone electron pairs are originally focused into the cavity. The monomethylated species *rac*-HMe-$(Q14N4Me_6)^{2+}$ is further remarkable in that the protonation occurs at an externally directed nitrogen atom, while the structure retains its initial skeletal form. The addition of the second methyl group results in a chemically induced rearrangement of the cis-fused tetracyclic skeleton, yielding a skeletal form that does not occur in the previously known systems. For the first time, a six membered ring having a boat conformation, rather than chair, has been observed in a Q14N4 based tetracycle structure. Similar exploitation of other substituted macrocycles is ongoing in our laboratories. Further, the $Cu^{2+}$ complexes of these ligands have been synthesized and characterized. They have familiar structures, and as expected, they exhibit exceptional kinetic stability due to the difficulty of stepwise donor dissociation of the *topologically constrained* cross-bridged ligands. Figure 2 provides a pictorial summary of the 13 known structures in the sequential syntheses of these complexes, including the 9 new structures first reported in this paper. We believe this degree of crystallographic characterization for a series of sequence-related intermediates, leading to the two closely related structurally characterized complexes, is rare and worth noting. This kind of crystallographic application to synthesis provides a productive synergism that must become more prevalent for these maturing sciences.

**Acknowledgment.** The authors are deeply appreciative of the generous support of this research by the Procter and Gamble Co. T.J.H. thanks the Madison and Lila Self-Graduate Fellowship of The University of Kansas for financial support. We thank the EPSRC and Siemens Analytical Instruments for grants in support of the diffractometer. The Kansas/Warwick collaboration was supported by NATO. H.J.C. thanks Memorial University of Newfoundland for sabbatical leave.

**Supporting Information Available:** Tables of atomic coordinates and equivalent isotropic displacement parameters, bond lengths and angles, anisotropic displacement parameters, hydrogen coordinates and isotropic displacement parameters, and experimental crystallographic details for the nine new X-ray crystal structures. This material is available free of charge via the Internet at http://pubs.acs.org.

IC990491S

(25) (a) Springborg, J.; Søtofte, I. *Acta Chem. Scand.* **1997**, *51*, 357. (b) Springborg, J.; Glerup, J.; Søtofte, I. *Acta Chem. Scand.* **1997**, *51*, 832.

(26) (a) Bianchi, A.; Garcia-España, E.; Micheloni, M.; Nardi, N.; Vizza, F. *Inorg. Chem.* **1986**, *25*, 4379. (b) Ciampolini, M.; Micheloni, M.; Vizza, F.; Zanobini, F.; Chimichi, S.; Dapporto, P. *J. Chem. Soc., Dalton Trans.* **1986**, 505. (c) Bencini, A.; Bianchi, A.; Borselli, A.; Ciampolini, M.; Garcia-España, E.; Dapporto, P.; Micheloni, M.; Paoli, P.; Ramirez, J. A.; Valtoncoli, B. *Inorg. Chem.* **1989**, *28*, 4279. (d) Bencini, A.; Bianchi, A.; Chimichi, S.; Ciampolini, M.; Dapporto, P.; Garcia-España, E.; Micheloni, M.; Nardi, N.; Paoli, P. *Inorg. Chem.* **1991**, *30*, 7.